This manuscript was accepted and published by ***Energy & Fuels***, a journal of the American Chemical Society. DOI: 10.1021/ef3002668 (http://dx.doi.org/10.1021/ef3002668).

This manuscript was placed into the present public repository with the consent of the Editor of *Energy & Fuels*. Publication data of the final, corrected work:

Trninić, M.; Wang, L.; Várhegyi, G.; Grønli, M.; Skreiberg, Ø.: Kinetics of corncob pyrolysis. Energy Fuels, **2012**, 26, 2005-2013. doi: 10.1021/ef3002668

Kinetics of Corncob Pyrolysis

Marta Trninić[†], *Liang Wang*[‡], *Gábor Várhegyi*[§,*], *Morten Grønli*[‡] *and Øyvind Skreiberg*[||]

[†] Department of Process Engineering, Faculty of Mechanical Engineering, University of Belgrade, Kraljice Marije 16, 11000 Belgrade, Serbia

[‡] Norwegian University of Science and Technology, Dept. of Energy and Process Engineering, Kolbjørn Hejes vei 1A, 7491 Trondheim, Norway

[§] Institute of Materials and Environmental Chemistry, Research Centre for Natural Sciences, Hungarian Academy of Sciences, PO Box 17, Budapest, Hungary 1525

[||] SINTEF Energy Research, Sem Saelands vei 11, 7465 Trondheim, Norway

[*] Corresponding Author. E-mail: varhegyi.gabor@ttk.mta.hu, Tel. +36 1 4381148, Fax: +36 1 4381147

ABSTRACT. Two different corncob samples from different continents and climates were studied by thermogravimetry at linear and nonlinear heating programs in inert gas flow. A distributed activation energy model (DAEM) with three and four pools of reactants (pseudocomponents) was used due to the complexity of the biomass samples of agricultural origin. The resulting models described well the experimental data. When the evaluation was based on a smaller number of experiments, similar model parameters were obtained which were suitable for predicting experiments at higher heating rates. This test indicates that the available experimental information was sufficient for the determination of the model parameters. The checks on the prediction capabilities were considered to be an essential part of the model verification. In another test the experiments of the two samples were evaluated together,

assuming more or less common kinetic parameters for both cobs. This test revealed that the reactivity differences between the two samples are due to the differences in their hemicelluloses and extractives. The kinetic parameter values from a similar earlier work on other biomasses (Várhegyi, G.; Bobály, B.; Jakab, E.; Chen, H. *Energy Fuels,* **2011**, *25,* 24-32.) could also been used, indicating the possibilities of a common kinetic model for the pyrolysis of a wide range of agricultural by-products.

Keywords: biomass; corncob; thermogravimetry; distributed activation energy model; *n*-order kinetics; kinetic regime.

1. Introduction

There is a growing interest in biomass fuels and raw materials due to climatic change problems. The thermal decomposition reactions play a crucial role during several of the biomass utilization processes. Thermogravimetric analysis (TGA) is a high-precision method for the study of the pyrolysis at low heating rates, under well defined conditions in the kinetic regime. It can provide information on the partial processes and reaction kinetics. On the other hand, TGA can be employed only at relatively low heating rates because the true temperature of the samples may become unknown at high heating rates. TGA has frequently been employed in the kinetic modeling of the thermal degradation of biomass materials. Due to the complex composition of biomass materials, the conventional linearization techniques of the non-isothermal kinetics are not suitable for the evaluation of the TGA experiments. Therefore the TGA experiments of biomass materials are usually evaluated by the non-linear method of least squares (LSQ), assuming more than one reaction.[1-5]

Biomass fuels and residues contain a wide variety of pyrolyzing species. Even the same chemical species may have differing reactivity if their pyrolysis is influenced by other species in their vicinity. The assumption of a distribution in the reactivity of the decomposing species frequently helps the kinetic evaluation of the pyrolysis of complex organic samples.[6] The distributed activation energy models (DAEM) have been used for biomass pyrolysis kinetics since 1985, when Avni et al. applied a DAEM

for the formation of volatiles from lignin.[7] The use of DAEM in pyrolysis research was subsequently extended to a wider range of biomasses and materials derived from plants.[8-18]

Due to the complexity of the investigated materials the model was expanded to simultaneous parallel reactions (pseudocomponents) that were described by separate DAEMs.[9-15,17-18] The increased number of unknown model parameters required least squares evaluation on larger series of experiments with linear and non-linear temperature programs.[9,15,17-18] The model parameters obtained in this way allowed accurate prediction outside of the domain of the experimental conditions of the given kinetic evaluations.[9,15,18] The prediction tests helped to confirm the reliability of the model.

The present work aims at testing the applicability of this approach on a biomass of high applicability potential. Corncob is a highly important agricultural by-product. The worldwide yearly corn production is around 800 million ton. The cob/grain ratio is estimated to be 12 - 20% on a dry basis.[19] The final report of a recent feasibility study[20] lists the advantages of corncob utilization as: "Cobs represent a small, 12% portion of corn stover remaining on the field and cob removal has negligible impact on organic carbon depletion from the soil; Cobs have limited nutrient value to the soil; … Cobs are collected at the combine discharge which avoids the inclusion of rocks and dirt in the biomass supply; … Whole and ground cobs have excellent flow properties and can be handled with conventional conveyors." Wang et al. recently examined the charcoal formation processes from three corncob samples.[21] Two of the samples from that study were analyzed further in the present work to discern the peculiarities of their decomposition kinetics. The models and evaluation strategies outlined in a recent work[18] were followed. Particular emphasize was taken to discern the similarities and differences between the behavior of the present samples and the kinetics established on other sorts of biomasses:[18] corn stalk, rice husk, sorghum straw, and wheat straw. The presently available works on the pyrolysis kinetics of corncobs[22-25] are far from the models and evaluation methods of the present work. As Aboyade et al. wrote recently in their work on corncob and sugar cane bagasse: "Normally, such multi-component analysis of biomass devolatilization kinetics is conducted via the model-fitting approach. However, in this study the Friedman's method has been applied ...".[25]

2. Samples and Methods

2.1. Samples. Grab samples of corncobs were obtained from Surcin, Belgrade's municipality in Serbia (ZP Maize Hybrid, ZP 505, denoted here as sample **S**), and Pioneer Hi-Bred International, Oahu, Hawaii (sample **P**). Their proximate and ultimate analyses as well as their heating values were shown in a recent work that investigated the charcoal yields from corncob.[21] Table 1 summarizes these analyses.

Table 1. Proximate and ultimate analyses of the samples[a]

	Proximate analysis			Ultimate analysis				
Sample	VM	fC	Ash	C	H	O[b]	N	S
Pcob	79.6	17.8	2.6	47.0	6.4	43.4	0.5	0.1
Scob	81.1	17.5	1.5	47.6	6.3	43. 9	0.6	0.2

[a] % (m/m), dry basis

[b] by difference

Note the different ash content of the **P** and **S** cobs: 2.6 and 1.5 % (m/m) on dry basis, respectively. The rest of the analysis data are similar for the two samples. The cobs were ground in a cutting mill mounted with a 1 mm sieve and stored at room temperature till the experiments.

2.2. Thermogravimetric experiments. The TGA measurements were performed by a Thermal Instruments TA Q600 thermobalance. Around 5 mg samples were spread on an alumina sample holder of ∅ 6 mm. The experiments were carried out in a nitrogen flow of 100 ml/min. The experiments started with a 30 min purging period at room temperature followed by a 30 min drying period at 105 °C. Each TGA experiment was normalized by the initial dry sample mass. For this purpose the sample mass measured at 120°C was selected. The sample mass normalized in this way is denoted by *m(t)*. Linear and stepwise heating programs were employed to increase the amount of information in the series of experiments.[4] The *T(t)* programs of the present work are shown in Figure 1. 5, 10 and 20°C heating

rates and a stepwise program were employed for both samples. The latter one was composed of 20°C/min heating ramps and isothermal sections of 30 minutes at 200, 250, 300, 350, 400, and 450°C.

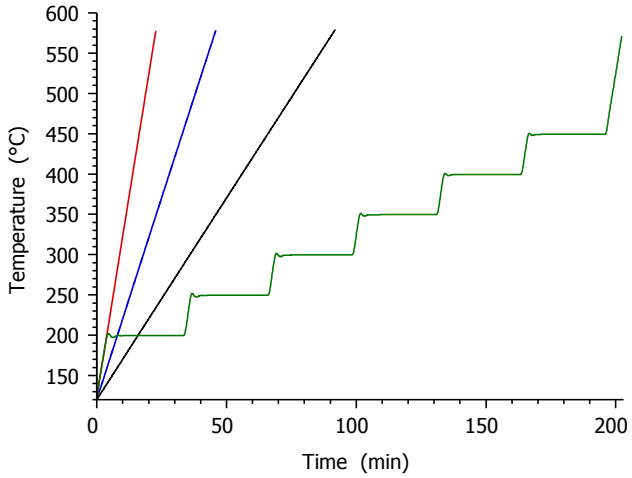

Figure 1. Temperature programs employed in the experiments: linear heating with heating rates of 20, 10 and 5 °C/min (red, blue and black lines, respectively) and a stepwise *T(t)* (green line).

2.3. Numerical methods. Fortran 95 and C++programs were employed for the numerical calculations and for graphics handling, respectively. The employed numerical methods have been described in details earlier.[18,26,27] The kinetic evaluation was based on the least squares evaluation of the -dm/dt curves. The method[28] used for the determination of -dm/dt does not introduce considerable systematic errors into the least squares kinetic evaluation of experimental results.[29]

3. Results and discussion

3.1. Evaluation by the method of least squares. The unknown model parameters were evaluated from series of 3 – 8 experiments by minimizing sum S_N where N is the number of experiments evaluated together:

$$S_N = \sum_{k=1}^{N} \sum_{i=1}^{N_k} \frac{\left[\left(\frac{dm}{dt} \right)_k^{obs} (t_i) - \left(\frac{dm}{dt} \right)_k^{calc} (t_i) \right]^2}{N_k h_k^{\,2}} \qquad (1)$$

Here subscript k indicates the experiments of the series evaluated. t_i denotes the time values in which the discrete experimental values were taken, and N_k is the number of the t_i points in a given experiment. h_k denotes the heights of the evaluated curves that strongly depend on the experimental conditions. The division by h_k^2 serves for normalization. The fit quality of the whole series was characterized by the following quantity:

$$fit_N\,(\%) = 100\ S_N^{0.5} \tag{2a}$$

When the fit quality of one experiment is characterized,

$$fit_1\,(\%) = 100\ S_1^{0.5} \tag{2b}$$

is calculated, where $S_1^{0.5}$ equals to the rms (root mean square) difference between the calculated and observed data normalized by the peak height (h) of the given experiment. Note that lower *fit* values indicate better fit qualities.

3.2. Distributed activation energy model (DAEM). As outlined in the *Introduction,* a model of parallel reactions with Gaussian activation energy distribution was chosen due to the favorable experience with this type of modeling on similarly complex materials.[9-15,17-18] According to this model the sample is regarded as a sum of M pseudocomponents, where M is usually between 2 and 4. Here a pseudocomponent is the totality of those decomposing species which can be described by the same reaction kinetic parameters in the given model. The number of reacting species is much higher than M in a complicated mixture of plant materials. The reactivity differences are described by different activation energy values. On a molecular level each species in pseudocomponent j is assumed to undergo a first-order decay. The corresponding rate constant (k) and mean lifetime (τ) are supposed to depend on the temperature by an Arrhenius formula:

$$k(T) = \tau^{-1} = \mathrm{A_j}\, e^{-E/RT} \tag{3}$$

Let $\alpha_j(t,E)$ be the solution of the corresponding first order kinetic equation at a given E and $T(t)$ with conditions $\alpha_j(0,E)=0$ and $\alpha_j(\infty,E)=1$:

$$d\alpha_j(t,E)/dt = A_j\, e^{-E/RT}\,[1-\alpha_j(t,E)] \tag{4}$$

The density function of the species differing by E within a given pseudocomponent is denoted by $D_j(E)$. $D_j(E)$ is approximated by a Gaussian distribution with mean $E_{0,j}$ and width-parameter (variation) σ_j. The overall reacted fraction of the jth pseudocomponent, $\alpha_j(t)$ is obtained by integration:

$$\alpha_j(t) = \int_0^\infty D_j(E)\ \alpha_j(t,E)\ \mathrm{d}E \tag{5}$$

The normalized sample mass, m, and its derivative are the linear combinations of $\alpha_j(t)$ and $\mathrm{d}\alpha_j/\mathrm{d}t$, respectively:

$$-\mathrm{d}m/\mathrm{d}t = \sum_{j=1}^{M} c_j d\alpha_j / dt \quad \text{and} \quad m(t) = 1 - \sum_{j=1}^{M} c_j \alpha_j(t) \tag{6}$$

where a weight factor c_j is equal to the amount of volatiles formed from a unit mass of pseudocomponent j.

3.3. The number of the pseudocomponents. Figure 2 compares the decomposition of the samples at 20°C/min heating rate. The main difference is the presence of a low temperature partial peak on the DTG curve of sample **P** with peak top at 231°C. This peak can be due to pectin which is a regular constituent of corncob; its typical abundance is about 3% (m/m).[30] The DTG peak temperature of untreated pectin is below 250 °C.[31,32] The rest of the decomposition is similar for the two cobs, though the hemicellulose and cellulose peaks occur at somewhat lower temperatures for the **P** cob. This can be due to the higher ash content of the **P** cobs, because some minerals may lower the peak temperatures of the hemicellulose and cellulose pyrolysis in agricultural by-products due to their catalytic activity. (See e.g. an early work on the pyrolysis of sunflower stems with different ash contents.[33]) Corncob **S** could be described well by assuming three pseudocomponents, in the same way as in an earlier work on agricultural residues with similar models and methods.[18] The model for the **P** cob, however, required an additional pseudocomponent for the low temperature peak. The parameters of this low temperature peak will be denoted by subscript 1: E_{01}, σ_1, A_1, and c_1.

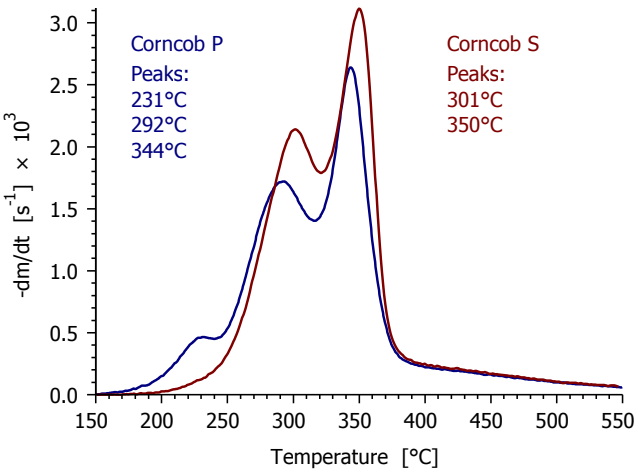

Figure 2. Comparison of the normalized mass-loss rate curves and peak temperatures of the two samples.

3.4. Prediction tests. Besides the quality of fit, an additional test was also used to check the validity of the models. In this test the experiments with the highest heating rate of the study were compared to predictions obtained from the evaluation of the slower experiments.[9,15,18] Such tests can be carried out for any type of kinetic modeling. The goodness of the model can be assessed by the fit quality and the prediction tests together. In the present work $fit_{20°C/\mathrm{min}}$ and $fit^{pred}_{20°C/\mathrm{min}}$ show the fit quality of the 20°C/min experiments in the regular evaluations, and in the prediction tests, respectively. The results will also be illustrated by figures later, in Sections 3.5 and 3.6. The difference of the parameters obtained from a smaller and a larger set of the experiments may be used to check the possibility of ill-definition problems in the evaluation. $\|\Delta E_0\|$, $\|\Delta\sigma\|$ and $\|\Delta c\|$ are the rms differences between the results of the evaluations based on the slower experiments and on all available experiments. The occurrence of a high value for $\|\Delta E_0\|$, $\|\Delta\sigma\|$ or $\|\Delta c\|$ would indicate that the lower number of the experiments is not sufficient for the unique determination of the kinetic parameters. However, none of the calculations with the DAEM model indicated such a problem in the present study. Table 2 lists these differences for the evaluations carried out on both 3 and 4 experiments. The evaluation of the **S** and **P** samples without special restrictions on the parameters, as described in the previous section, are rows S1 and P1 in this table. The rest of the evaluations will be explained in the next section. The highest $\|\Delta E_0\|$ in the table,

10 kJ/mol belongs to evaluation S1. Note that similar uncertainties (standard deviations of 8-10 kJ/mol) were observed in a round-robin study on pure cellulose samples that were evaluated by simple first order kinetics.[34] The $\|\Delta\sigma\|$ and $\|\Delta c\|$ values are negligible in Table 2. The differences between the $fit_{20°C/min}$ and $fit^{pred}_{20°C/min}$ values are also low indicating that the prediction tests and the regular least squares evaluations resulted in similar fit qualities for the 20°C/min experiments.

However, these observations do not mean that three experiments are always enough for the unique determination of 12 – 16 kinetic parameters. Figure 2 indicates that the hemicellulose and cellulose peaks are well separated in the present samples; accordingly the experiments contain ample information for the determination of the corresponding kinetic parameters. These peaks highly overlap each other in many agricultural residues and other materials of plant origin.[17,18,29,33] The merging of two peaks rises the possibility of more than one mathematical solutions that describes the experiments equally well.[14,17,18]

Table 2. Separate evaluation of corncobs S and P by DAEM reactions[a]

No.	Values taken from a work on other biomasses[18]	$\frac{N_{param}}{N}$	fit_4 (%)	$fit_{20°C/min}$ (%)	$fit^{pred}_{20°C/min}$ (%)	$\|\Delta E_0\|$ (kJ/mol)	$\|\Delta\sigma\|$ (kJ/mol)	$\|\Delta c\|$
S1	none	3	1.9	2.4	2.9	10	0.8	0.002
S2	E_0 , σ	1.5	2.5	3.5	3.7	–	–	0.007
S3	E_0 , σ, A	0.8	4.1	5.4	5.5	–	–	0.003
P1	none	4	1.7	1.7	2.0	3	0.2	0.002
P2	E_{02}, E_{03}, E_{04}, σ_2,σ_3, σ_4	2.5	2.2	2.6	2.8	1[b]	0.3[b]	0.002
P3[c]	E_{02}, E_{03}, E_{04}, σ_2,σ_3, σ_4 A_2, A_3, A_4	1	6.3	7.1	7.2	–	–	0.004

[a] S1, S2, S3 are evaluations of sample **S** assuming three partial reactions. P1, P2, P3 are evaluations of sample **P** assuming four partial reactions. Each partial reaction is described by DAEM kinetics. $fit_{20°C/min}$ and $fit^{pred}_{20°C/min}$ shows the fit quality of the 20°C/min experiments in the regular evaluations, and in the prediction tests, respectively. Lower *fit* values mean better fit qualities. $\|\Delta E_0\|$, $\|\Delta\sigma\|$ and $\|\Delta c\|$ are the rms differences between the results of the evaluations based on four and three experiments, as described in the text.

[b] Difference between the parameters of the first peak only (because the corresponding values of the other peaks were not changed).

[c] Here the kinetic parameters of the low-temperature peak (A_1, E_{01}, and σ_1) were taken from evaluation P2, as described in the text.

3.5. Describing corncob pyrolysis kinetics by parameters obtained for other sort of agricultural residues. The next step in the modeling was the clarification of the similarities and differences between the present corncob samples and other agricultural residues that were studied by the same models and evaluation techniques in a preceding work: corn stalk, rice husk, sorghum straw, and wheat straw.[18] In that work the different agricultural residues were described by more or less common kinetic parameters. Common E_0 and σ were searched for the corn stalk, rice husk, sorghum straw, and wheat straw in one of the approaches employed.[18] In this case the shape and width of the partial curves were identical. The preexponential factors however, depended on the type of the biomass. At given E_0 and σ values the increase of the preexponential factor moves the corresponding partial curve to a lower temperature. In this way the preexponential factors can express the different amounts of catalytic minerals in the

different biomasses. The c_j weight factors of eq. 6, which define the sizes (areas) of the partial peaks, also differed for the biomasses hence the c_j values expressed the compositional differences between the biomasses. The E_0 and σ values obtained in this approach were used as constants in evaluations S2 and P2 of the present work. The results obtained so are shown in rows S2 and P2 of Table 2 and columns S2 and P2 of Table 3. The E_{02}, E_{03}, E_{04}, σ_2, σ_3 and σ_4 values taken from the earlier work are listed in Table 3. The low temperature peak did not occur in corn stalk, rice husk, sorghum straw, and wheat straw samples; hence E_{01} and σ_1 were free parameters in evaluation P2.

The use of predefined, constant parameters obviously decreases the number of free parameters, N_{param}. For a comparison with the evaluations from higher number of experiments, the ratios of N_{param} and the number of experiments evaluated (N) is shown in Table 2.

In another approach of the earlier work[18] all kinetic parameters were assumed to be common for corn stalk, rice husk, sorghum straw, and wheat straw. Such A, E_0 and σ values were searched which were applicable for the four materials together. In this method the differences between the biomasses were expressed only by the c_j weight factors of eq. 6, which define the sizes (areas) of the partial peaks. The A, E_0 and σ values obtained in this way were used as constants in evaluations S3 and P3 of the present work. The corresponding results are shown in rows S3 and P3 of Table 2 and columns S3 and P3 of Table 3. The values taken from the earlier work are A_2, A_3, A_4, E_{02}, E_{03}, E_{04}, σ_2, σ_3 and σ_4 in Table 3, as noted there in a table footnote. In Evaluation P3 the free variation of the kinetic parameters of the low temperature peak resulted in a false convergence, accordingly the E_{01}, σ_1 and A_1 values of evaluation P2 were employed in evaluation P3 as constants. Accordingly only the c_i factors were varied in S3 and P3, as the low N_{param}/N indicates in Table 2.

Table 3. List of the model parameters for seven selected evaluations

Model	DAEM		DAEM		DAEM		DAEM		*n*-order	
Evaluation[a]	S2	P2	S3	P3	DAEM2		DAEM3		n_order3	
Sample	**S**	**P**	**S**	**P**	**S**	**P**	**S**	**P**	**S**	**P**
Figures	**3a**	**3c**	**3b**	**3d**	–	–	**4a**	**4c**	**5a**	**5c**
fit_8 / %	2.1		5.3		1.9		2.4		2.5	
E_{01} / kJ mol^{-1}	–	142	–	142[b]	–	141	–	141	–	138
E_{02} / kJ mol^{-1}	177[c]		176[c]		180[d]		180[d]		173[d]	
E_{03} / kJ mol^{-1}	185[c]		185[c]		196[d]		187[d]		186[d]	
E_{04} / kJ mol^{-1}	194[c]		189[c]		205[d]		225[d]		261[d]	
σ_1 / kJ mol^{-1}	–	0.1	–	0.1[b]	–	1.3	–	2.7	–	–
σ_2 / kJ mol^{-1}	4.3[c]		7.1[c]		4.2[d]		3.9[d]		–	–
σ_3 / kJ mol^{-1}	1.9[c]		1.7[c]		0.0[d]		0.2[d]		–	–
σ_4 / kJ mol^{-1}	34.6[c]		32.7[c]		29.2[d]		31.3[d]		–	–
$\log_{10} A_1$ / s^{-1}	–	13.25	–	13.25[b]	–	13.11	–	13.01	–	12.77
$\log_{10} A_2$ / s^{-1}	14.45	14.79	14.13[c]		14.75	15.10	14.76	15.02	14.20	14.44
$\log_{10} A_3$ / s^{-1}	13.87	13.96	13.71[c]		14.80	14.90	14.11[d]		14.00[d]	
$\log_{10} A_4$ / s^{-1}	12.98	13.3	13.9[c]		14.50	14.72	16.25[d]		19.52[d]	
n_1	–	–	–	–	–	–	–	–	–	2.14
n_2	–	–	–	–	–	–	–	–	1.90[d]	
n_3	–	–	–	–	–	–	–	–	0.94[d]	
n_4	–	–	–	–	–	–	–	–	10.38[d]	
c_1	–	0.04	–	0.03	–		–	0.05	–	0.07
c_2	0.24	0.21	0.33	0.28	0.25	0.21	0.23	0.21	0.29	0.25
c_3	0.37	0.31	0.30	0.21	0.33	0.27	0.34	0.29	0.32	0.27
c_4	0.17	0.17	0.13	0.18	0.18	0.18	0.20	0.16	0.19	0.14

[a] See Tables 2 and 4 for the meaning of these abbreviations

[b] E_{01}, σ_1 and A_1 had fixed values in Evaluation P3. (They were taken from Evaluation P2.)

[c] Values taken from an earlier work on other biomasses[18] as explained in the text

[d] Parameters forced to have the same values for samples **S** and **P**.

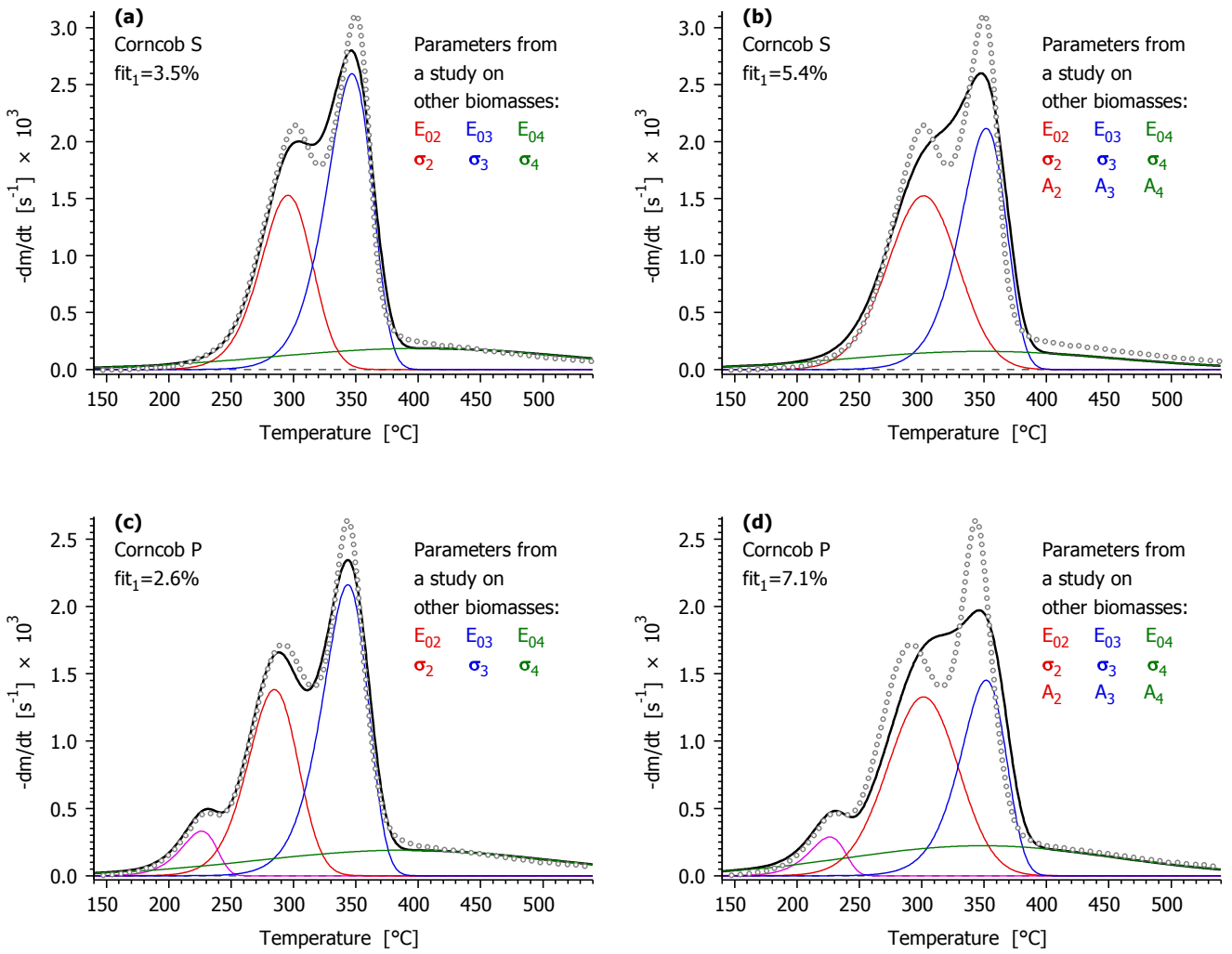

Figure 3. Evaluations by DAEM kinetics. Part of the kinetic parameters were taken from an earlier work on agricultural biomasses.[18] (See evaluations S2, S3, P2 and P3 in Tables 2 and 3.) Four experiments were evaluated simultaneously for each sample and the 20°C/min experiments are shown here. Notation: observed mass loss rate curve (gray circles); its calculated counterpart (black solid line); and partial reactions (thin solid lines of different colors).

The partial curves and the fit quality is shown for the S2, P2, S3 and P3 evaluations at 20 °C/min heating rate in Figure 3. The first, low temperature peak of magenta color occurs only in sample **P**, and was identified as pectin decomposition, as outlined above. The second and third peaks (red and blue colors) are due to hemicellulose and cellulose pyrolysis, respectively. The last process (color green in

the figures) in a very wide temperature domain describes the lignin decomposition as well as the slow carbonization of the chars formed in the pyrolysis.[18] These are only approximate assignments, however; because more than one biomass component can contribute to a given pseudocomponent. (See the definition of the term pseudocomponent in Section 3.2.)

Plots (a) and (c) in the left-hand-side of Figure 3 display a reasonable fit quality. However, the calculated curves (black solid lines) show too high overlap in plots (b) and (d) of Figure 3 because the preexponential factors were not allowed to vary in the corresponding evaluations. Accordingly the rms differences between the observed and calculated points are higher here, as the fit_1 values in the graphic fields indicate. Nevertheless, these calculated curves with lower fit quality still can be employed as models with rougher approximation. The omission of the low temperature peak from the model of the **P** cobs results only in a moderate worsening of the fit quality: fit_4 increases to 6.8 from 6.3% while $fit_{20°C/min}$ changes from 7.1 to 7.5 %. These observations suggest that it is possible to describe a wide range of biomass materials in a rough approximation by a common model of three partial DAEM reactions in which only the areas of the partial peaks differ.

3.6. Describing the two corncob samples by common kinetic parameters. The next step in the modeling was the clarification of the similarities and differences between the two corncob samples. For this purpose the eight experiments of the two samples were evaluated simultaneously and the number of common parameters values were gradually increased. The processes and the characteristics of the performance of the evaluations are summarized in Table 4. The notation is similar to that of Table 2 except that the present quantities are calculated from the corresponding values of the **S** and **P** cobs together. Hence fit_8 shows the fit quality of the eight experiments together; $fit_{20°C/min}$ are the root mean square of the fit_1 values of the 20°C/min experiments on the **S** and **P** cobs; $fit^{pred}_{20°C/min}$ is a similar value calculated from the prediction tests, and $||\Delta E_0||$, $||\Delta\sigma||$ and $||\Delta c||$ are rms differences between the values determined from all experiment (8 experiments) and from the slower experiments (6 experiments). The $||\Delta n||$ values belong to the n-order kinetics that will be discussed in the next section. The first row

contains the characteristics calculated from the separate evaluations of the samples (Evaluations S1 and P1 that were shown in Table 2, too). The assumption of common E_{02}, E_{03}, E_{04} and σ_2, σ_3, σ_4 values for samples **S** and **P** only slightly changed the performance of the modeling, as the rows DAEM1 and DAEM2 show in Table 4. In a further test the preexponential factors of the cellulose decomposition (A_3) and the wide, flat peak (A_4) were also assumed to be common in the two samples. Row DAEM3 in Table 4 and Figure 4 show that this model variant still produced an acceptable performance. Figure 4 displays the 20°C/min experiments. Plots (a) and (c) in the left-hand-side of Figure 4 belong to the regular least squares evaluation of the eight experiments while plots (b) and (d) show the prediction from the six slower experiments as described in paragraph 3.4.

The assumptions of evaluation DAEM3 mean that the main difference between the pyrolysis kinetics of samples **S** and **P** lies in the existence of the small low temperature peak in corncob **P** and the in different reactivity of the hemicellulose. The rest of the decomposition (cellulose, lignin and the slow carbonization processes of the char) can be described by identical kinetic parameters for both cobs.

When a further parameter, A_2 was also set to be equal in the two samples, the fit quality and the stability of the evaluation worsened. (This version is not shown in Table 4.)

Table 4. Simultaneous evaluation of samples S and P[a]

Evalu-ation	Parameters with identical values in both samples	$\frac{N_{param}}{N}$	fit_8 (%)	$fit_{20°C/min}$ (%)	$fit^{pred}_{20°C/min}$ (%)	$\|\Delta E_0\|$ (kJ/mol)	$\|\Delta\sigma\|$ (kJ/mol)	$\|\Delta n\|$	$\|\Delta c\|$
S1 & P1	none	3.5	1.8	2.0	2.4	7	0.5	–	0.002
DAEM1	E_{02}, E_{03}, E_{04}	3.1	1.9	2.2	2.6	1	0.4	–	0.004
DAEM2	E_{02}, E_{03}, E_{04}, σ_2, σ_3, σ_4	2.8	1.9	2.2	2.6	4	0.5	–	0.004
DAEM3	E_{02}, E_{03}, E_{04}, σ_2, σ_3, σ_4, A_3, A_4	2.5	2.4	3.0	3.3	4	0.7	–	0.003
n_order1	E_{02}, E_{03}, E_{04}	3.1	2.0	2.0	2.7	14	–	4.3	0.125
n_order2	E_{02}, E_{03}, E_{04}, n_2, n_3, n_4	2.8	2.0	2.3	2.7	2	–	0.5	0.07
n_order3	E_{02}, E_{03}, E_{04}, n_2,n_3, n_4, A_3, A_4	2.5	2.5	3.1	3.4	3	–	0.4	0.08

[a] Simultaneous evaluation of 8 experiments assuming four partial reactions. The first partial reaction (a low temperature peak) occurs only in sample **P**. $fit_{20°C/min}$ and $fit^{pred}_{20°C/min}$ show the rms fit qualities of the two 20°C/min experiments in the regular evaluations and in the prediction tests, respectively. $\|\Delta E_0\|$, $\|\Delta\sigma\|$, $\|\Delta n\|$, and $\|\Delta c\|$ are the rms differences between the results of the evaluations based on eight and six experiments, as described in the text.

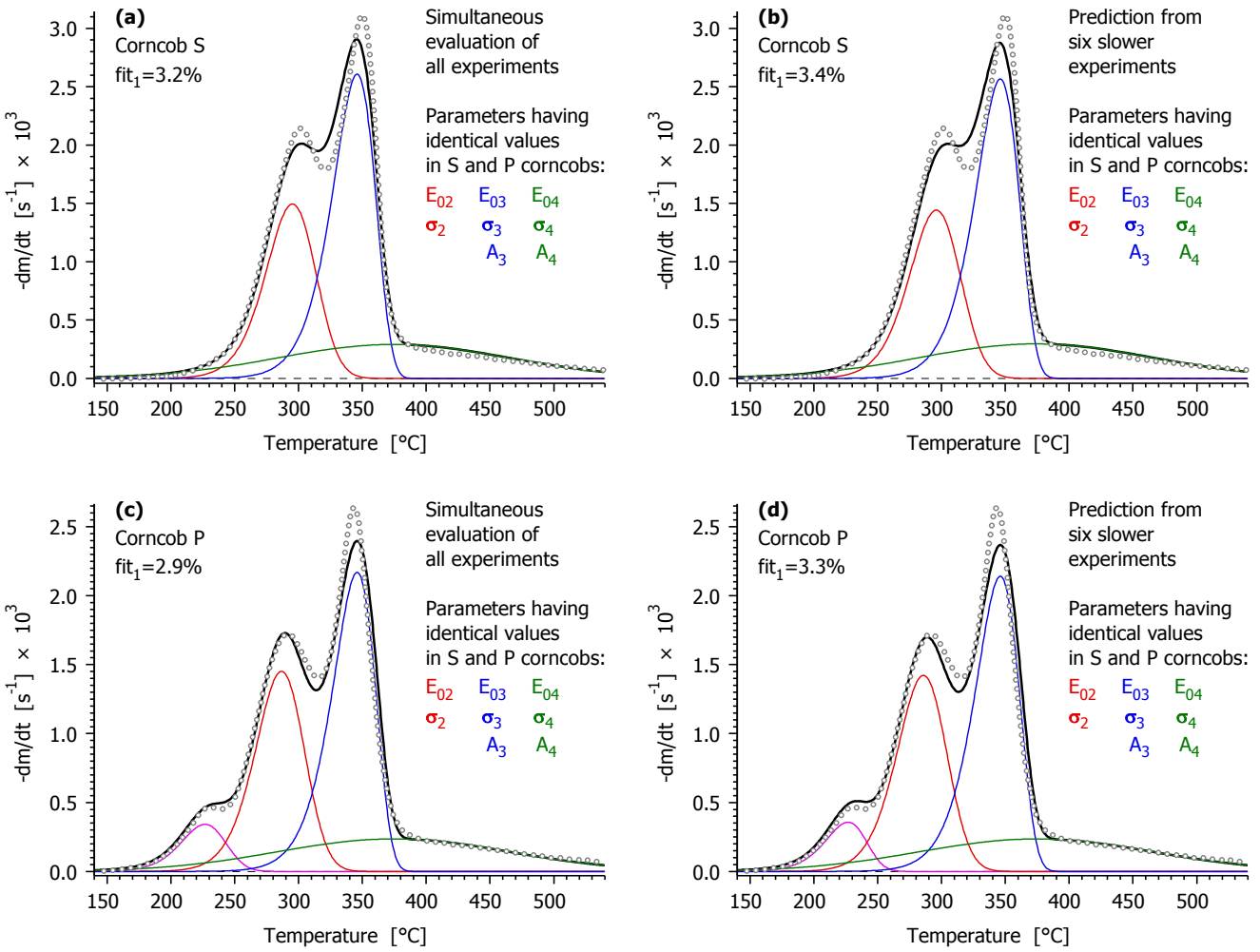

Figure 4. Evaluation by DAEM kinetics assuming eight common parameters for the two samples. The fit quality and partial curves of the 20°C/min experiments are shown. The left-hand-side (plots **a** and **c**) belongs to the regular least squares evaluation of the eight available experiments while the right-hand-side (plots **b** and **d**) displays the prediction from the six slower experiments. See Figure 3 for notations. The parameter values and other details are listed in Tables 3 and 4 at evaluation "DAEM3".

3.7. Tests with *n*-order kinetics. The *n*-order kinetics has the same number of model parameters as the DAEM with Gaussian distribution, while its numerical solution is simpler and faster. To test this approach, evaluations similar to DAEM1, DAEM2 and DAEM3 were carried out with *n*-order kinetics. The corresponding evaluations are denoted in Tables 3 and 4 by n_order1, n_order2 and n_order3. The

assumptions on common σ_2, σ_3, and σ_4 in evaluations DAEM2 and DAEM3 were replaced by assumptions on common n_2, n_3, and n_4 in evaluations n_order2 and n_order3. The partial curves and fit qualities of the 20°C/min experiments for evaluation n_order3 and the results of the corresponding prediction tests are shown in Figure 5 in the same way as it was done in the case of evaluation DAEM3 in Figure 4.

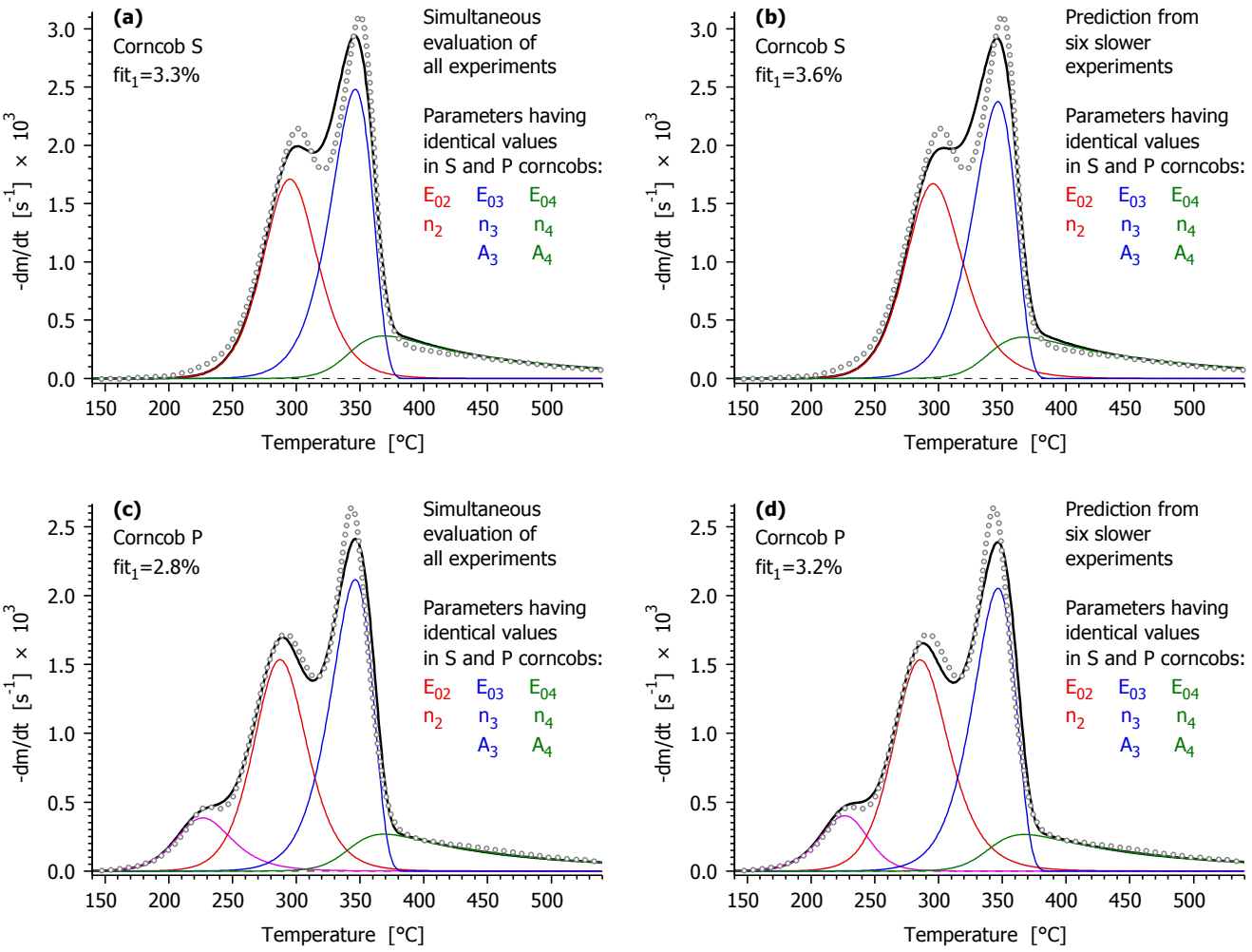

Figure 5. Evaluation by *n*-order kinetics assuming eight common parameters for the two samples. The fit quality and partial curves of the 20°C/min experiments are shown. The left-hand-side (plots **a** and **c**) belongs to the regular least squares evaluation of the eight available experiments while the right-hand-side (plots **b** and **d**) displays the prediction from the six slower experiments. See Figure 3 for notations. The parameter values and other details are listed in Tables 3 and 4 for evaluation "n_order3".

The data of Table 4 shows that similar fit qualities can be obtained by the *n*-order model. The prediction tests also gave similar results. The comparison of the kinetic parameters obtained from six and eight experiments revealed high $||\Delta c||$ differences, especially for evaluation n_order1, accordingly the DAEM model has better-defined parameters during the evaluation. Besides, the *n*-order kinetics describes the complexity of the biomass materials in a rather formal way while a DAEM gives a simplified, but clear picture on the different reactivities of the different biomass species. The faster numerical calculation has little importance keeping in mind the low price and high speed of the desktop computers nowadays.

3.8. Notes on the obtained kinetic parameter values. Evaluations S2 and P2 in the left hand side of Table 3 used those E_{02}, E_{03}, E_{04}, σ_2, σ_3, σ_4 values that was obtained from the evaluation of corn stalk, rice husk, sorghum straw, and wheat straw samples together in a preceding work.[18] In that work common E_0 and σ parameters were assumed for different biomasses. In the present work evaluation DAEM2 assumed common E_0 and σ parameters for two different samples. The E_0 values of evaluation DAEM2 are similar to the values of the earlier work; the highest difference is 11 kJ/mol (ca. 6%). The σ_2 and σ_3 values are also very close: the difference in σ_2 and σ_3 are 0.1 and 1.9 kJ/mol, respectively. Note that the low σ_3 values indicate a nearly first order cellulose decomposition. When σ_3=0, the corresponding DAEM reaction is exactly equivalent to the first order kinetics (because the Gaussian distribution is a Dirac delta function). The assumption of common A_3 and A_4 in evaluation DAEM3 only slightly changed the kinetic parameters. Note that the approximation by *n*-order kinetics also resulted in similar activation energies for three of the four partial reactions, as the data of evaluation n_order3 indicated in Table 3. The reaction order observed for the cellulose decomposition is near to first order (n_3=0.94), in accordance with the σ_3=0 value of the DAEM approach.

The presented kinetic parameters describe the behavior in a wide range of experimental conditions, and proved to be suitable for predictions. Besides part of the parameters (E_{02}, E_{03}, E_{04}, σ_2, σ_3, σ_4)

proved to be close to or were identical with the values obtained for other agricultural residues, as described above. Based on these observations, we think that the outlined model gives a reliable account on the kinetics.

On the other hand, an important aim of the kinetics is to produce sub-models that can be coupled with transport phenomena to describe practical conversion systems.[35] The coupling itself is obviously easier with models consisting of a few first order reactions. A problem with the first order kinetics, however, is that the activation energy is nearly inversely proportional to the peak width of the DTG curves at linear heating.[36] Accordingly the flat, wide pyrolysis sections appearing at linear heating result in low formal activation energy values in the models based on first order kinetics. Activation energies down to 18 kJ/mol were reported in several studies.[37] This problem does not arise in the DAEMs because DAEMs can describe wide, flat peaks with realistic magnitudes of activation energies. There are possibilities, however, to obtain reasonable approximations with two or three first order partial reactions. An obvious approximation possibility is to disregard the long, tailing sections (which occur above 400°C in the figures of the present article) because the evaluation of such flat section results in low activation energies. Besides, the activation energies of the remaining processes can be forced to trustworthy ranges by mathematical constraints. The work of Branca et al.[38] employs such approaches and presents simple, but useful approximate models for wood devolatilization. However, we believe that the high developing rate of the computers and computing methods will make possible the use of the more complex kinetic sub-models, too, in the future. According to the present state of the literature and to our own experience in the field, the first order models need considerable higher number of partial reactions than the DAEMs to describe a wide range of observations with a comparable precision in biomass pyrolysis.[15] In the present wok and its predecessor[18] a particular emphasis was taken to keep the ratio of the unknown model parameters and the number of experiments low so that the evaluation would yield well defined, dependable kinetic parameters that can be employed for different agricultural by-products.

4. Conclusions

(i) The pyrolysis of corncob samples was studied by a model of DAEM partial reactions at linear and stepwise heating programs. Four pseudocomponents were used corresponding to the thermal decomposition of pectin (1); hemicelluloses (2); cellulose (3); and a wide, low reaction rate process that involved the lignin decomposition and the slow carbonization of the formed chars (4).

(ii) The pyrolysis of two different corncob samples from different continents and climates were found similar except that the small pectin peak occurred only in one of the samples and some reactivity differences arose in the hemicellulose pyrolysis. When the experiments of the two samples were evaluated together, the following parameters required different values in the two samples: the weight factors of the partial peaks (c_j) and the preexponential factor of the hemicellulose (A_2). Note that the lack of the pectin peak corresponds to c_1=0 in the model. Eight parameters (E_{02}, E_{03}, E_{04}, σ_2, σ_3, σ_4, A_3, and A_4) could be assumed identical in the two samples without a notable worsening of the fit quality.

(iii) The parameter values obtained at the joint evaluation of other biomass samples (corn stalk, rice husk, sorghum straw, and wheat straw) in an earlier work[18] were similar to their counterparts of the present work. The values from the earlier work proved to be applicable for the corncob model, too. When the E_0 and σ values were employed as fixed parameters, high fit quality was observed. When the A values of the earlier work were also included as fixed parameters, a rougher, but still usable approximation was obtained. These observations suggest that it is possible to construct common models for wide ranges of biomass materials. If a rough approximation is enough then only the parameters related to the sample compositions (c_j) should be varied from biomass to biomass.

(iv) When n-order kinetics was employed instead of the DAEM partial reaction, similar fit qualities were obtained. However, the n-order kinetics describes the complexity of the biomass materials in a rather formal way while a DAEM gives a simplified, but clear picture on the different reactivities of the different biomass species.

(v) All the results in this work were checked by prediction tests. In these tests 20°C/min experiments were simulated by the model parameters obtained from the evaluation of the experiments with stepwise *T(t)* and linear *T(t)* with slower heating rates.

Acknowledgment. The authors acknowledge the financial support by the Bioenergy Innovation Centre (CenBio), which is funded by the Research Council of Norway, a large number of industry partners and seven R&D institutions. G. Várhegyi is grateful for the support of the Hungarian National Research Fund (OTKA K 72710).

NOMENCLATURE

α_j	reacted fraction of a pseudocomponent (dimensionless)
A_j	pre-exponential factor (s^{-1})
c_j	normalized mass of volatiles formed from a pseudocomponent (dimensionless)
E_{0j}	mean activation energy in a distributed activation energy model (kJ/mol)
fit_N	fit quality calculated for a group of N experiments by equation 2 (%)
$fit_{20°C/min}$	fit quality calculated for the 20°C/min experiments (%)
h_k	height of an experimental curve (s^{-1})
k	rate constant (s^{-1})
m	normalized sample mass (dimensionless)
N	number of experiments in a given evaluation
N_k	number of evaluated data on the kth experimental curve
R	gas constant (8.3143×10^{-3} kJ mol^{-1} K^{-1})
rms	root mean square
σ_j	width parameter (variance) of the Gaussian distribution (kJ/mol)
S_N	least squares sum for N experiments (dimensionless)
t	time (s)

T temperature (°C, K)

τ mean lifetime of a species

Subscripts:

i digitized point on an experimental curve

j pseudocomponent

k experiment

REFERENCES

(1) Várhegyi, G.; Antal, M. J., Jr.; Székely, T.; Szabó, P. Kinetics of the thermal decomposition of cellulose, hemicellulose and sugar cane bagasse. *Energy Fuels* **1989**, *3*, 329-335.

(2) Manyà, J. J.; Velo, E.; Puigjaner, L. Kinetics of biomass pyrolysis: a reformulated three-parallel-reactions model. *Ind. Eng. Chem. Res.,* **2003**, *42*, 434 -441.

(3) Branca, C.; Di Blasi C. Global intrinsic kinetics of wood oxidation. *Fuel* **2004**, *83*, 81-87.

(4) Várhegyi, G. Aims and methods in non-isothermal reaction kinetics. *J. Anal. Appl. Pyrolysis* **2007**, *79*, 278-288.

(5) Conesa, J. A.; Domene, A. Biomass pyrolysis and combustion kinetics through n-th-order parallel reactions. *Thermochim. Acta*, **2011**, *523*, 176-181.

(6) Burnham, A. K.; Braun, R. L. Global kinetic analysis of complex materials. *Energy Fuels* **1999**, *13*, 1-22.

(7) Avni, E.; Coughlin, R. W.; Solomon P. R., King H. H. Mathematical modelling of lignin pyrolysis. *Fuel* **1985**, *64* 1495-1501.

(8) Reynolds, J. G.; Burnham, A. K.; Wallman, P. H. Reactivity of paper residues produced by a hydrothermal pretreatment process for municipal solid wastes. *Energy Fuels* **1997**, *11*, 98-106.

(9) Várhegyi, G.; Szabó, P.; Antal, M. J., Jr. Kinetics of charcoal devolatilization. *Energy Fuels* **2002**, *16*, 724-731.

(10) de Jong, W; Pirone, A; Wojtowicz, M. A. Pyrolysis of Miscanthus Giganteus and wood pellets: TG-FTIR analysis and reaction kinetics. *Fuel,* **2003**, *82*, 1139-1147.

(11) Wójtowicz, M. A.; Bassilakis, R.; Smith, W. W.; Chen, Y.; Carangelo, R. M. Modeling the evolution of volatile species during tobacco pyrolysis. *J. Anal. Appl. Pyrolysis*, **2003**, *66*, 235-261.

(12) Yi, S-C.; Hajaligol, M. R. Product distribution from the pyrolysis modeling of tobacco particles. *J. Anal. Appl. Pyrolysis*, **2003**, *66*, 217-234.

(13) Yi, S-C.; Hajaligol, M. R.; Jeong, S. H. The prediction of the effects of tobacco type on smoke composition from the pyrolysis modeling of tobacco shreds. *J. Anal. Appl. Pyrolysis*, **2005**, *74*, 181-192.

(14) de Jong, W.; Di Nola, G.; Venneker, B. C. H.; Spliethoff, H.; Wójtowicz, M. A. TG-FTIR pyrolysis of coal and secondary biomass fuels: Determination of pyrolysis kinetic parameters for main species and NO_x precursors. *Fuel,* **2007**, *86*, 2367-2376.

(15) Becidan, M.; Várhegyi, G.; Hustad, J. E.; Skreiberg, Ø. Thermal decomposition of biomass wastes. A kinetic study. *Ind. Eng. Chem. Res.* **2007**, *46*, 2428 - 2437.

(16) Sonobe, T.; Worasuwannarak, N. Kinetic analyses of biomass pyrolysis using the distributed activation energy model. *Fuel* **2008**, *87*, 414-421.

(17) Várhegyi, G.; Czégény, Zs.; Jakab, E.; McAdam, K.; Liu, C. Tobacco pyrolysis. Kinetic evaluation of thermogravimetric - mass spectrometric experiments. *J. Anal. Appl. Pyrolysis* **2009, *86*, 310-322.**

(18) Várhegyi, G.; Bobály, B.; Jakab, E.; Chen, H. Thermogravimetric study of biomass pyrolysis kinetics. A distributed activation energy model with prediction tests. *Energy Fuels,* **2011**, *25,* 24-32.

(19) Maung, T. A.; Gustafson, C. R. The viability of harvesting corn cobs and stover for biofuel production in North Dakota. **2011,** AAEA & NAREA Joint Annual Meeting, July 24-26, 2011, Pittsburgh, Pennsylvania, The full text is available at http://ageconsearch.umn.edu/bitstream/103613/2/AAEAPaper2_050211.pdf

(20) Chippewa Valley Ethanol Company (CVEC). Corn cobs as sustainable biomass for renewable energy, a field-to-facility demonstration and feasibility study. Final Report to the Minnesota Department of Commerce Office of Energy Security, 2009. Available at: http://www.auri.org/research/CVEC_Final_Report_to_Office_of_Energy_Security_30.pdf

(21) Wang, L.; Trninic, M.; Skreiberg, O.; Morten, G.; Considine, R.; Antal, M. J. A. Is elevated pressure required to achieve a high fixed-carbon yield of charcoal from biomass? Part 1: Round-robin results for three different corncob materials. *Energy Fuels* **2011**, *25*, 3251–3265.

(22) Chen, Y.; Duan, J.; Luo, Y. Investigation of agricultural residues pyrolysis behavior under inert and oxidative conditions. *J. Anal. Appl. Pyrol.* **2008**, *83*, 165-174.

(23) Yu, F.; Ruan, R.; Steele, P. Consecutive reaction model for the pyrolysis of corn cob. *Transact. ASABE* **2008**, *51*, 1023-1028.

(24) Zabaniotou. A.; Ioannidou, O.; Antonakou, E.; Lappas, A. Experimental study of pyrolysis for potential energy, hydrogen and carbon material production from lignocellulosic biomass. *Internat. J. Hydrogen Energy* **2008**, *33*, 2433-2444.

(25) Aboyade, A. O.; Hugo, T. J.; Carrier, M.; Meyer, R. L.; Stahl, R.; Knoetze, J. H.; Görgens, J. F. Non-isothermal kinetic analysis of the devolatilization of corn cobs and sugar cane bagasse in an inert atmosphere. *Thermochim. Acta* **2011**, *517*, 81-89.

(26) Várhegyi, G.; Czégény, Zs.; Liu, C.; McAdam, K.: Thermogravimetric analysis of tobacco combustion assuming DAEM devolatilization and empirical char-burnoff kinetics. *Ind. Eng. Chem. Res.,* **2010**, *49*, 1591-1599.

(27) Donskoi, E.; McElwain, D. L. S. Optimization of coal pyrolysis modeling. *Combust. Flame* **2000**, *122*, 359-367.

(28) Várhegyi, G.; Till, F. Computer processing of thermogravimetric - mass spectrometric and high pressure thermogravimetric data. Part 1. Smoothing and differentiation. *Thermochim. Acta* **1999**, *329*, 141-145.

(29) Várhegyi, G.; Chen, H.; Godoy, S. Thermal decomposition of wheat, oat, barley and *Brassica carinata* straws. A kinetic study. *Energy Fuels* **2009**, *23*, 646-652.

(30) Bagby, M. O.; Widstrom, N. W. Biomass uses and conversions. in *Corn: Chemistry and Technology* (edited by Watson, S. A; Ramstad, P.E). American Association of Cereal Chemists, Inc., St. Paul, MN, **1987**, 575-590.

(31) Fisher, T.; Hajaligol, M.; Waymack, B.; Kellogg, D. Pyrolysis behavior and kinetics of biomass derived materials. *J. Anal. Appl. Pyrolysis* **2002**, *62*, 331-349.

(32) Einhorn-Stolla, U.; Kunzeka, H.; Dongowski G. Thermal analysis of chemically and mechanically modified pectins. *Food Hydrocolloids* **2007**, *21*, 1101–1112.

(33) Várhegyi, G.; Jakab, E.; Till, F.; Székely, T. Thermogravimetric - mass spectrometric characterization of the thermal decomposition of sunflower stem. *Energy Fuels* **1989**, *3*, 755-760.

(34) Grønli, M.; Antal, M. J., Jr.; Várhegyi, G. A round-robin study of cellulose pyrolysis kinetics by thermogravimetry. *Ind. Eng. Chem. Res.* **1999**, *38*, 2238-2244.

(35) Di Blasi, C. Modeling chemical and physical processes of wood and biomass pyrolysis. *Progr. Energy Combust. Sci.*, **2008**, *34,* 47-90.

(36) Várhegyi, G.; Székely, T. Reaction kinetics in thermal analysis: The sensitivity of kinetic equations to experimental errors. A mathematical analysis. *Thermochim. Acta* **1982**, *57*, 13-28.

(37) Garcìa-Pèrez, M.; Chaala, A.; Yang, J.; Roy, C. Co-pyrolysis of sugarcane bagasse with petroleum residue. Part I: thermogravimetric analysis. *Fuel* **2001**, *80*, 1245-1258.

(38) Branca, C.; Albano A.; Colomba Di Blasi, C. Critical evaluation of global mechanisms of wood devolatilization. *Thermochim*. *Acta* **2005**, *429*, 133-141.